STRIATUS 2.0
PHOENIX – IMPROVING CIRCULARITY OF 3D-CONCRETE-PRINTED UNREINFORCED MASONRY STRUCTURES

ALESSANDRO DELL'ENDICE / SERBAN BODEA / TOM VAN MELE / PHILIPPE BLOCK
BLOCK RESEARCH GROUP, ETH ZÜRICH
VISHU BHOOSHAN / SHAJAY BHOOSHAN / HEBA EIZ / TAIZHONG CHEN
COMPUTATION & DESIGN GROUP (CODE), ZAHA HADID ARCHITECTS
HÉLÈNE LOMBOIS-BURGER / LOIC REGNAULT DE LA MOTHE / SERGE NANA
HOLCIM INNOVATION CENTER
JOHANNES MEGENS / SANDRO SANIN
INCREMENTAL3D
THEO BÜRGIN
BÜRGIN CREATIONS

Introduction

This paper describes the realisation of Striatus 2.0: Phoenix, a permanent, 3D-concrete-printed, dry-assembled, unreinforced-masonry arched footbridge composed of dry-assembled, 3D-concrete-printed blocks (Fig. 1). The research presented in this paper details the improvements that were made to the novel integrated design, engineering, and fabrication framework and to the manufacturing and assembly processes used in the realisation of Striatus (Bhooshan *et al.*, 2022a, b; Dell'Endice *et al.*, 2023). This paper builds on the relevance of the computational masonry paradigm to deliver the ecological promises of 3D concrete printing (3DCP) and provides a detailed comparison between the two iterations of the bridge (Figs. 2, 3).

State of the art

Relevant precedent 3DCP structures are: the very first 3DCP pedestrian bridge installed at the Institute for Advanced Architecture of Catalonia (IAAC), Barcelona (IAAC, 2016; IAAC, Acciona, 2017; Wangler *et al.*, 2019), bicycle bridges in Gemert (Salet *et al.*, 2018) and Nijmegen, both in the Netherlands (van der Kley *et al.*, 2018), and a pedestrian bridge in Shanghai, China (Xu *et al.*, 2020). It can be noted that none of them use the unreinforced-masonry (URM) paradigm (Bhooshan *et al.*, 2023). The URM design and construction techniques are perfectly compatible with the compression-dominant, orthotropic material properties of layered 3D-printed concrete. For an in-depth review, we refer the reader to Bhooshan (2023) and Dell'Endice *et al.* (2023).

Rapid urbanisation and climate change heightens the urgency of addressing the circularity of building construction (Wangler *et al.*, 2019; Block *et al.*, 2020; Fivet and Brütting, 2020). In this context, the widespread and relatively cheap availability of concrete, the low cost of the technological requirements for its use, and its beneficial material properties make it an important material. However, given the expected high-volume use of concrete in the immediate future, it is vital to mitigate the associated carbon emissions (Monteiro *et al.*, 2017). Decarbonisation of the concrete industry is critically important.

The Striatus bridge

The Striatus bridge (2021) was designed to be installed, dismantled, reassembled, and repurposed, demonstrating how the four Rs of circularity (reduce, reuse, repair,

1

recycle) can be applied to concrete structures. See Bhooshan *et al.* (2022a, b), and Dell'Endice *et al.* (2023). The following lessons were learned:

1. The size of the 3DCP blocks challenged transportation and manoeuvrability during the assembly. Improved alignment strategies are needed.
2. The assembly strategy adopted, from the supports towards the centre, lacked a strategic approach to close the resulting gaps when placing the keystones.
3. The assembly relied entirely on the precision of the falsework. Some errors in its design led to imprecisions. Additionally, an improved strategy to reduce single-use materials for the centring and increase reusable parts is needed.
4. The 3DCP process involved inherent tolerances that were not quantified. As a result, the real block length was not cross-referenced with its digital counterpart, introducing an additional layer of uncertainty that, in turn, impacted the accuracy of the assembly.
5. The 3DCP blocks were fabricated using high-strength (90MPa) concrete with aggregates measuring less than 1mm. Transitioning to larger aggregates would reduce the percentage of cement in the mix, while using lower-strength concrete would enhance the use of recycled raw materials in the cement recipe.

The transition from Striatus to Phoenix considered all these issues and challenges. It aimed at enhancing the structure's sustainability by focusing on three objectives: (i) optimising the carbon footprint, (ii) reducing the reliance on virgin resources through improved circularity, and (iii) extending the structure's design life.

Striatus 2.0: Phoenix bridge

Phoenix, being the second iteration of Striatus, builds on the collaborative, multi-author design-to-production (DTP) toolchain described in Bhooshan *et al.* (2022a), and Dell'Endice *et al.* (2023), with the improvements in each thread detailed below.

Architectural and structural design

The geometry of Phoenix is shallower than that of Striatus (Fig. 2). It is better suited for a pedestrian footbridge and does not require steps. The number of blocks has been increased to improve manoeuvrability and adjustment and reduce transportation requirements (Fig. 4), leading to a new assembly system detailed in Assembly strategy. Reducing the dimensions and weight of the blocks promoted their compressive-only behaviour, discouraging bending stresses (Ranaudo *et al.*, 2022). The reduction in the height of the balustrade blocks gave Phoenix a lighter

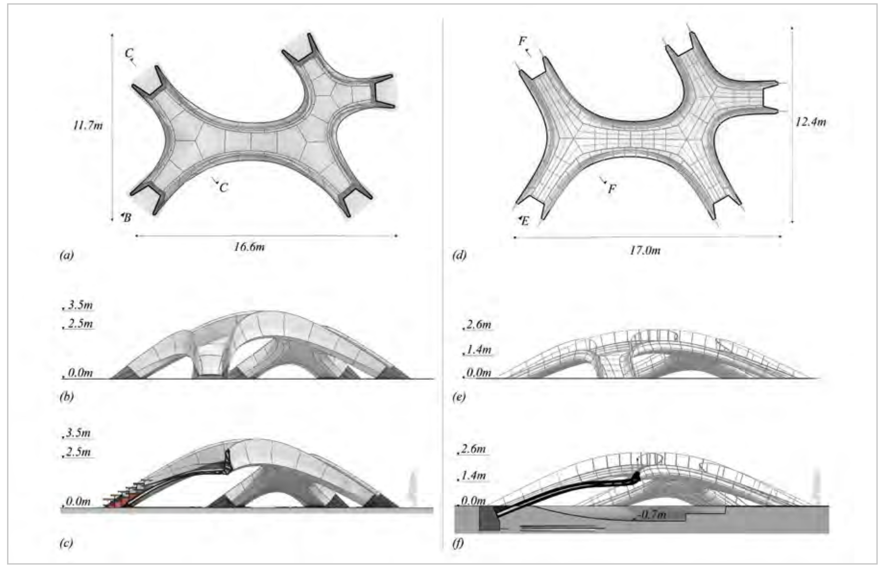

2


3

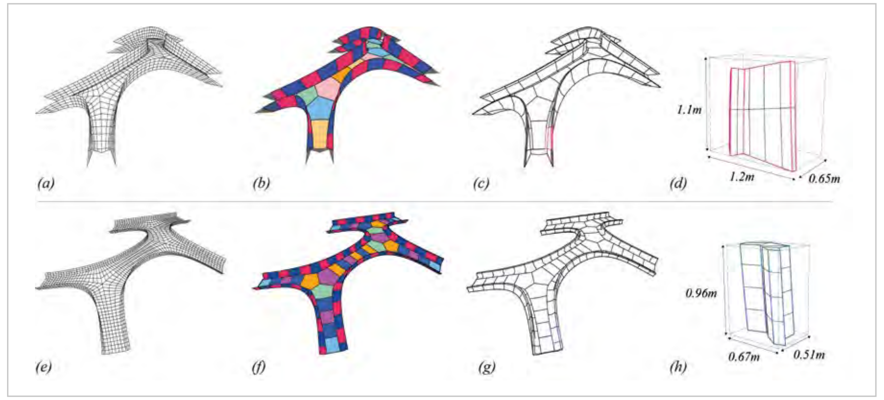

4

1. Completed Phoenix bridge at the Holcim Innovation Center, Lyon, France. © Alessandro Dell'Endice.

2. Schematic drawings showing the shallower arch design and less deep balustrade blocks of the Phoenix (right) versus the Striatus (left) bridge.

3. The Striatus bridge exhibited at the Giardini della Marinaressa, Venice, Italy, in 2021. © Naaro.

4. Striatus (top) versus Phoenix (bottom): (a–c) versus (e–g) compare the block subdivision; (d) and (h) compare a typical balustrade block.

5. Detail of the handrail installed on a T-shaped steel element inserted between neoprene pads at the interface. © Cecilia Vuillermoz.

appearance compared with Striatus and required the development of a handrail system, clamped between the blocks, taking advantage of the thrust of the arch (Fig. 5). The structural design also involved the internal stiffening schemes of the blocks, as described in Print-path synthesis. Since the deck blocks only require curvature in the spanning direction along the bridge's skeleton and laterally receive compression forces from the balustrade arches, the cross-section in the short direction does not need curvature. In other words, there is no arch action in the short direction of the bridge. Consequently, the internal stiffening scheme, to reduce the free span of the deck blocks' horizontal top and bottom layers, was simplified and reduced to vertical stiffeners only. With the intention of designing a permanent structure, a few expedients were adopted to improve the robustness of the system:

1. The structural depth of the deck blocks was increased, which enlarges the equilibrium solution space for live load cases.
2. The cross-section at the base of the balustrade blocks was increased.
3. In the cross-section of the 3DCP components, the printed layers were thicker (nominal thickness 48mm), avoiding double layers with potentially imperfect bonding.
4. The shallow geometry reduced the curvature variation in each 3D-printed block, namely the angle between the start and end printing planes, making the layer height variation in a single component less extreme.

The structural design of Phoenix closely followed Striatus, comprising three phases. First, form-finding was conducted using thrust network analysis (TNA) (Block, 2009). Subsequently, materialisation, discretisation, global equilibrium, and displacement capacity were accomplished using the Discrete Element Modelling (DEM) method, through *compas_3dec*, which uses the software 3DEC by Itasca as a solver in the background (Dell'Endice, 2023). Lastly, local stress assessments were carried out using finite element modelling (FEM) analysis.

Structural analysis

For Phoenix, SLS and ULS load combinations, differential settlements, thermal loads, creep analysis, snow, wind, and horizontal loads according to the Eurocode were applied using the FEM software ABAQUS. The FEM analysis was conducted on the discretised model, allowing the formation of hinges/openings at the joints. The average compressive stress experienced with SLS simulations was only 2.65MPa, with a peak of 5.2MPa

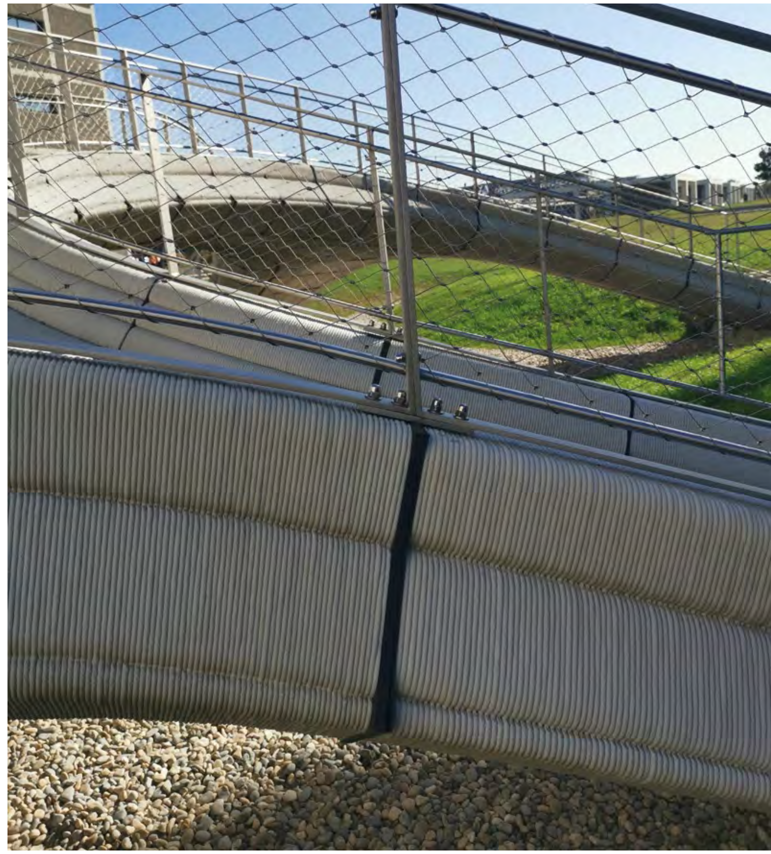
5

in just one loading case. For ULS, the average calculated compressive stresses were 5MPa, with a peak of 9.3MPa in only one loading configuration. These results confirmed that compression stresses are not an issue, being a mere one-tenth of the nominal compressive capacity of the 2K ink employed (50MPa) and one-fifth of its design strength after considering safety factors. As expected, the funicular geometry and informed discretisation, i.e., stereotomy, of the structure play a significant role in maintaining remarkably low compressive stress levels within the structure.

The design of the individual 3D-printed components also paid attention to the tensile strength of the printed material. The 2K ink used for Phoenix has a nominal tensile strength of only 2.85MPa and a design tensile strength equivalent to 2.28MPa (for SLS) and 1.52MPa (for ULS). The FEM analysis has shown that, for SLS loading conditions, the structure experiences average tensile stresses equal to 1MPa and, only in one case, 1.8MPa. For ULS configurations, the structure experiences, on average, 1.39MPa with peaks of 1.5MPa, remarkably close to the ULS tensile strength equal to 1.52MPa.

Print-path synthesis
The cross-section of the deck blocks was updated from a triangular bracing to vertical stiffeners. The dual-layer print path used in Striatus was also updated to a single-layer print path with double the print width (48mm), which halved the overall print length (29km). The so-called signed distance fields (SDFs), used to generate the print paths, were updated accordingly. For both the deck and balustrade blocks, the initial procedure to compute the base profile from the interpolated print planes remains the same. The resultant SDF (f_{result}) constitutes the Boolean of four individual SDFs, each serving a specific purpose:

- base profile polygon f_o
- offset polygon $f_1 = f_o + 0.5 * \textit{print width}$; f_1 controls the cross-sectional print thickness based on specified print width and f_o
- brace f_2 = *line SDF at brace points;* f_2 provides local stiffeners in each cross-section
- trim f_3 = *perpendicular line SDF of brace;* f_3 aids in the creation of one continuous print profile
- resultant $f_{result} = (f_1 - f_2) \cup (f_3)$

Typical bottlenecks in the computational time of SDFs (Erleben and Dohlmann, 2008) were alleviated by using GPU-based parallel computing. It accelerated the computational production time and increased the field resolution for greater control of output contours and faster generation of the print paths for all the blocks: 112 minutes for Striatus (53 blocks, single thread CPU) versus 1.8 minutes for Phoenix (104 blocks, GPU).

The feature-based sampling procedure described in Bhooshan *et al.* (2022b) was used in the post-processing stage to create one contiguous print path from the SDF contours, which have uneven sampling. The maximum sampling distance in Phoenix was increased from 10mm to 15mm to reduce the total number of points supplied to the robot, while still having minimal deviation from the block geometry. Varying print widths were used based on the outer and inner segments created by the feature points.

Material development
To address the material's sustainability targets, a custom-made, proprietary TectorPrint ink was developed for the project. As explained in Architectural and structural design, the design improvements relaxed the requirements on the layer thickness and width. In general, the narrower the layers, the higher the required material strength and consequently the material CO2eq footprint, as the water-to-binder ratio and the admissible maximum particle size are reduced. While Striatus was based on a 90MPa micro mortar with 1mm maximum size sand, in Phoenix, because of the 24mm print width, the layer width was increased to 48mm such that a 50 MPa mortar with 2mm maximum size sand could be used. The circularity of the mix was improved by using a fully recycled cement, type CEM III/A 42.5 N, with clinker made entirely of recycled minerals (Holcim lance le premier clinker 100% recyclé au monde, 2022) in combination with slag, and demolition sand from Striatus included in the dry mortar fraction.

Altogether, this resulted in a third of the ink coming from recycled materials. Furthermore, the CO2eq footprint of the ink was optimised by increasing the proportion of local material through the use of local sand (sourced 15km from the printing facility), which meant that half of the ink was made up of local materials. The local sand was mixed with the reduced dry mortar fraction in the printing facility when preparing the successive batches of ink, to feed the robot.

A 2K technology was used to ensure optimum processability, so that:

- The material is still fluid at the end of the batch mixing, with ad-hoc slump retention during the duration of batch consumption for printing.
- Buildability of the structure is tuned on demand, depending on printing speed requirements, by a secondary admixture (optimised in this project for the selected binder) introduced in the printhead where it is mixed just prior to printing with the fluid material fed from the batch mixer.

Outside building codes, 3D printing brings certain challenges (potential weakness of interfaces between layers, risk in curing due to the absence of formworks, so that drying starts from material deposition). As a result, the in-situ performance of the ink was checked both on samples cut from prints and on structural elements. Each structural test was run twice, with good consistency of results and sizeable safety margins.

Fabrication
By reducing the block size, the printing process benefited from removing the raft prints, necessary in Striatus due to larger blocks with higher curvature (Bhooshan *et al.*, 2022b). Another pertinent change was the thicker monolithic external layer, while the internal bracings were established with thinner parallel/double layers.

While the print paths for the Striatus blocks were designed in parallel layers, for Phoenix, monolithic outer layers of 48mm thickness were applied. Compared with Striatus, the GCode definition was expanded to include layer-width parameters per target in order to align robotic speed and the required material volume per target. To establish a continuous path, the internal bracings were established as parallel layers at half the width of the outer layers, which allowed Phoenix to place material as required (Fig. 6). The omission of raft layers enabled the blocks to be packed for transport immediately after curing, eliminating the additional step of raft removal.

Overall, the print time for all blocks was 67 hours, compared with 84 hours for Striatus, while the weight of both bridges is similar (around 25t). Next to time savings due to the avoidance of raft prints, a higher rate of mortar flow in the extrusion process of 3.2l/min accelerated production.

6. 3D printing of a block with a monolithic external layer. © incremental3D.

7. Crane lifting of the cassette falsework system with blocks preassembled. © Cecilia Vuillermoz.

8. Placement of one cassette on the scaffolding system. © Cecilia Vuillermoz.

9. Dismantling the scaffolding and falsework system after decentring. © Alessandro Dell'Endice.

6

7

8

9

Assembly strategy
The falsework and assembly logic of Striatus were entirely reworked. The new objective was to enhance assembly precision while minimising single-use falsework components. The bridge was dry assembled with neoprene pads inserted at each block interface to avoid stress concentrations or assembly misalignments. The base of the falsework system consisted of standard scaffolding towers positioned along the central axis of the bridge, while the waffle system was divided into separated components called cassettes (Fig. 8).

To reduce the number of custom, single-use components, the depth of the waffle and the number of elements were minimised, while standard steel beams were introduced as part of the waffle's structure, reducing the volume per m^2 of timber by 50%. By working per cassette, the lighter

10

11

blocks could be precisely arranged with the neoprene pads in between. Thereafter, the cassettes were lifted onto the scaffolding towers and registered in the right place following predefined measurements (Fig. 7).

Assembly followed a predefined sequence, starting from the centre and working towards the supports, where a gap of 2.5cm was left from the foundations (Fig. 8). This strategy was adopted to control the fabrication tolerances and assembly imprecisions in the sensitive middle, and to lump them at the last interface with the supports, where they could be compensated by filling the resulting gap with mortar, after the assembly and before the decentring. After the decentring, the structure successfully underwent a structural test, where four different loading cases were simulated by adding sandbags to the deck area.

Circularity and sustainability

3D-printing ink
From Striatus to Phoenix, the ink was optimised from a C90/105 to a C50/60 mortar, using a local and coarser sand, mixed with a dry mortar premix (the latter including demolition sand) in the printing factory. As a result, the amount of recycled material in the ink reached one-third of the weight.

Altogether, a footprint reduction of 40% CO2eq per m^3 of the 3DCP ink was achieved, mostly stemming from the decline in the strength category of the material. In detail, reducing the nominal compressive strength from 90MPa to 50MPa had an impact of one-third on the global CO2eq savings, using coarser and local sand one-quarter, using a low-carbon cement two-fifths; the route optimisation had an impact of one-sixth as well.

Comparison of the two footbridges
Both versions were compared in terms of carbon footprint. Rescaling accounted for difference in span (14m for Striatus, 16m for Phoenix) and deck surface ($43m^2$ for Striatus, $53m^2$ for Phoenix). The latter was chosen as the functional unit, and therefore Striatus was rescaled to a $53m^2$ deck surface area. Excluding the foundations, which are in both cases not representative and/or optimised solutions, the results show a 25% reduction of the carbon footprint, with the following key evolutions of the footprints:

- 34% reduction for the {deck + balustrade}
- 60% increase for the elastomer joints
- 62% reduction for the formwork
- 100% reduction of the cover footprint

However, a diminished CO2eq footprint is just one aspect of the overall picture. As mentioned in the introduction, this bridge is designed as a permanent structure and engineered for circularity, a factor not considered in the carbon calculations.

Future research
Future research in the domain of 3DCP and URM structures offers a wide range of avenues for exploration and improvement, including:

1. Enhancing material performance in tension
2. Rethinking interfaces
3. Innovating the activation mechanism
4. Integrating circularity in carbon footprint assessment
5. Refining measurement and reference systems

10. Completed 3DCP block assembly in preparation for handrail installation. © Cecilia Vuillermoz.

11. Intrados close-up of the completed Phoenix bridge at the Holcim Innovation Centre, Lyon, France. © Alessandro Dell'Endice.

Conclusion

The Phoenix bridge represents a significant research advancement in URM structural logic applied to 3DCP, addressing critical challenges encountered in Striatus, focusing on circular construction, environmental impact reduction, and structural robustness.

Advancements include: the sustainability of the concrete ink which incorporates recycled aggregates from the disassembled Striatus blocks, overall structural performance, optimising the print-path synthesis and 3D-printing process, minimising material waste, and devising an assembly strategy that maximises standardised off-the-shelf components, reducing the need for custom-made, single-use parts.

The Phoenix bridge project represents a significant advancement in applying 3DCP and URM principles for sustainable construction. It offers valuable insights into circular construction practices and environmental impact reduction while pushing the boundaries of this innovative technology.

Acknowledgements

Additional credits: Jianfei Chu, Henry David Louth, Efthymia Doroudi, Patrik Schumacher (ZHA); Vasilis Aloutsanidis (BRG); Fulei Zhou, Sandrine Reboussin, Sylvain Duchand, Bilal Baz, Cyril Chiale, Christian Blachier, Marjorie Chantin-Coquard, Alain Dunand, Mickaël Peraud, Fabien Sandra, Adrien Moulin, Emmanuel Bonnet (Holcim); Georg Grasser, Thomas Badegruber, Nikolas Janitsch, Janos Mohacsi, Marcel Hiller, Thomas Koger (in3D); Martin Jucker, Semir Mächler (Bürgin Creations); Ibrahim Alachek, Jeremy Ouedraogo, Gianluca Cardia (Amodis).

References

Bhooshan, S., Bhooshan, V., Dell'Endice, A., Chu, J., Singer, P., Megens, J., Van Mele, T. and Block, P. (2022a) The Striatus bridge: Computational design and robotic fabrication of an unreinforced, 3D-concrete-printed, masonry arch bridge. *Architecture, Structures and Construction*, 2(4), pp.521-543.

Bhooshan, S., Bhooshan, V., Megens, J., Casucci, T., Van Mele, T. and Block, P. (2022b) Print-path design for inclined-plane robotic 3D printing of unreinforced concrete. *Design Modelling Symposium Berlin*, pp.188-197. Cham: Springer.

Bhooshan, S., Dell'Endice, A., Ranaudo, F., Van Mele, T. and Block, P. (2024) Unreinforced concrete masonry for circular construction. *Architectural Intelligence*, 3(7). https://doi.org/10.1007/s44223-023-00043-y.

Bhooshan, S. 2023. Shape design of 3D-concrete-printed masonry structures. ETH Zürich. https://doi.org/https://doi.org/10.3929/ethz-b-000614010.

Block, P. (2009) *Thrust Network Analysis: Exploring three-dimensional equilibrium*, PhD thesis, MIT Department of Architecture.

Block, P., Van Mele, T., Rippmann, M., Ranaudo, F., Calvo Barentin, C.J. and Paulson, N. (2020) Redefining structural art: Strategies, necessities and opportunities. *The Structural Engineer*, 98(1), pp.66-72.

Dell'Endice, A., Bouten, S., Van Mele, T. and Block, P. (2023) Structural design and engineering of Striatus, an unreinforced 3D-concrete-printed masonry arch bridge. *Engineering Structures*, 292, p.116534. https://doi.org/10.1016/j.engstruct.2023.116534.

Dell'Endice, A. (2023) Structural assessment and design of unreinforced masonry structures using discrete element modelling. https://doi.org/10.3929/ETHZ-B-000596377.

Erleben, K. and Dohlmann, H. (2008) Signed distance fields using single-pass gpu scan conversion of tetrahedra. *Gpu Gems*, 3, pp.741-763.

Fivet, C. and Brütting, J. (2020) Nothing is lost, nothing is created, everything is reused: Structural design for a circular economy. *The Structural Engineer*, 98(1), pp.74-81.

Holcim lance le premier clinker 100% recyclé au monde. (2022) Lafarge France: Ciment, Bétons, Granulats, Solutions Et Produits [Preprint]. https://www.lafarge.fr/holcim-lance-le-premier-clinker-100-pour-cent-recycle-au-monde.

IAAC (2016) IAAC 3DCP bridge. https://iaac.net/wp-content/uploads/2018/10/Press-Release-IAAC-3D-printed-bridge-1.pdf.

IAAC, Acciona (2017) IAAC and ACCIONA. URL https://www.archdaily.com/804596/worlds-first-3d-printed-bridge-opens-in-spain.

Monteiro, P.J., Miller, S.A. and Horvath, A. (2017) Towards sustainable concrete. *Nature Materials*, 16(7), pp.698-699.

Ranaudo, F., Van Mele, T. and Block, P. (2022) On the thrust line of piecewise-linear-elastic continuous funicular structures. In: *Proceedings of the IASS/APCS 2022 Symposium*, Beijing.

Salet, T., Ahmed, Z., Bos, F. and Laagland, H. (2018) Design of a 3D printed concrete bridge by testing. *Virtual and Physical Prototyping*, 13(3), pp.222-236. https://doi.org/10.1080/17452759.2018.1476064.

van der Kley, M., TU Eindhoven and Witteveen+Bos (2018) The Bridge Project. https://www.bridgeproject.nl/english/project/.

Wangler, T., Roussel, N., Bos, F.P., Salet, T.A. and Flatt, R.J. (2019) Digital concrete: A review. *Cement and Concrete Research*, 123, p.105780.

Xu, W., Gao, Y., Sun, C. and Wang, Z. (2020) Fabrication and application of 3D-printed concrete structural components in the Baoshan Pedestrian Bridge project. In: Burry, J., Sabin, J., Sheil, B. and Skavara, M. eds., *FABRICATE 2020: Making Resilient Architecture*. London: UCL Press, pp140-148.